

THE TWERLE BALLOON-TO-SATELLITE  
DATA TRANSMITTING SYSTEM

Nadav Levanon, Juris Afanasjevs, Scott D. Ellington, Robert A. Oehlkers, Verner E. Suomi  
Space Science and Engineering Center, The University of Wisconsin, Madison, Wisconsin

Ernest W. Lichfield and Michael W. Gray  
National Center for Atmospheric Research, Boulder, Colorado

Abstract

This paper describes the balloon instrumentation system which provides the one-way link for data gathering and navigation in the Tropical Wind, Energy conversion and Reference Level Experiment (TWERLE). In this experiment 400 instrumented constant-level balloons will be launched at the southern hemisphere during 1975. The Random Access Measurement System (RAMS) on board the NIMBUS-F satellite, will comprise the receiving end of the link.

The data encoder, stable oscillator, transmitter and antenna are described, as well as two supporting components, the power source and the magnetic cutdown. These six items weigh 850 g. The oscillator-transmitter consume 1.9 W dc power to provide 0.6 W phase modulated RF power. Standby dc power consumption is 0.3 W.

Introduction

In 1975 four-hundred constant altitude meteorological balloons will be launched in the southern hemisphere as part of the Tropical Wind, Energy conversion and Reference Level Experiment (TWERLE). Each balloon will transmit one-second data bursts, once per minute, during daytime hours. The data will be received by the Random Access Measurements System (RAMS) on board the NIMBUS-F satellite. The balloon position will be reconstructed from the varying Doppler shift recorded on board the satellite during an overpass. The balloons will float at an altitude of approximately 14 km for a period of up to 6 months, circling the globe about once per month.

Each balloon carries three sensors which measure altitude, temperature, and pressure. A fourth parameter, the wind, is deduced from the balloon positions.

The transmitter specifications imposed by the RAMS system are as follows:

Nominal Frequency	401.2 + 0.003 MHz	
Frequency Stability	10 <sup>-8</sup> /15 min	long term
	10 <sup>-8</sup> /1 s	short term
	2 x 10 <sup>-6</sup> /6 month	aging
RF Power	0.6 W	
Modulation	+ 60° ± 6°	
Modulation Symmetry	5°	
Modulation Rate	100 bits/s	(Manchester)

Antenna: Semihemispheric Pattern  
Polarization: Circular (right hand)  
Gain at 5° elevation >0 dB  
Gain at 80° elevation >-15 dB

The original frequency spread will be increased by an additional spread of ± 8.2 KHz due to the Doppler shift, and a frequency spread due to aging. The total frequency spread cannot exceed the ± 15 KHz bandwidth of the satellite receiver.

Determination of accurate winds requires reception

from at least two consecutive overpasses. For a balloon near the equator, which happens to get an exact overhead pass, the previous, or next, path will be seen for 4 min at above 5° elevation. Unfortunately, the low elevation path has also the longest path-length and the worst direction in respect to the satellite single lobe antenna. These considerations led to the antenna specification above.

Packaging of electronics for ballooning is unique from all other forms of electronic packaging. Packaging considerations are as follows:

- Minimization of weight - of prime importance  
(from both balloon load and frangibility aspects)
- Miniaturization of size - not desirable unless it reduces weight
- Thermal design - very important

The thermal design of the package is very important, as each package is exposed to the flight environment and must provide an acceptable internal temperature. This is usually accomplished by using the sun as a heat source and choosing the package shape, absorption, emissivity and insulation to give the desired internal temperature. It should be pointed out that while the ambient temperature is between -50°C to -80°C, the inside temperature of a dark object may reach high temperatures due to solar radiation.

Shock and vibration are not important considerations. Once the electronics are at float, accelerations are essentially non-existent. All that is necessary is that the equipment be sturdy enough to withstand handling, shipping, and launch.

Frangibility is an important design criteria. Since there is a slight chance of collision with aircraft during balloon ascent, it is required that the electronics be fabricated so that they would do minimal damage to an aircraft. A design goal for the packaging of the TWERLE electronics is that the mass density per unit area in any direction of impact be less than 2 grams per cm<sup>2</sup>. This is less than the mass density of a large bird. To meet this low impact density requirement, the electronics are separated into many small assemblies that are mechanically and electrically interconnected by lightweight wire.

A photograph of a TWERLE balloon and flight train is presented in Fig. 1 which was taken during a test flight in Christchurch, New Zealand in February 1974. (The corner reflector below the balloon is not a standard part of the TWERLE flight train.) A schematic of the flight train is given in Fig. 2. The various components of the flight train will be discussed in the following sections except for the three sensors which will be described in separate papers elsewhere.

Data Encoder

The control point for the entire balloon flight train is the Data Encoder package, an electronic

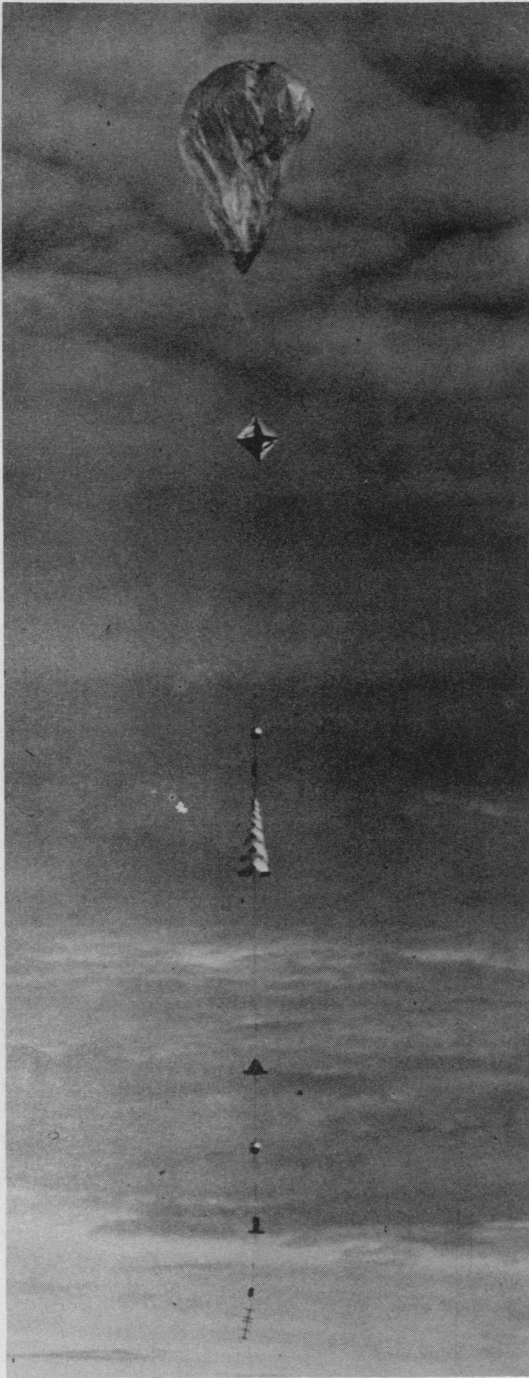


Fig. 1. TWERLE flight train  
(Christchurch, New Zealand, 2 March 1974)

assembly which includes the following system functions:

- Timing of the system
- Digitizing of sensor inputs
- Generating of fixed format bit patterns
- Combining of fixed format with digitized sensor data
- Generating Manchester-coded modulation format to drive transmitter
- Power and control switching of sensors and transmitters.

Fig. 3 is the block diagram for the TWERLE Data Encoder. The majority of the circuits are designed using COS/MOS logic from the RCA 4000 series. The

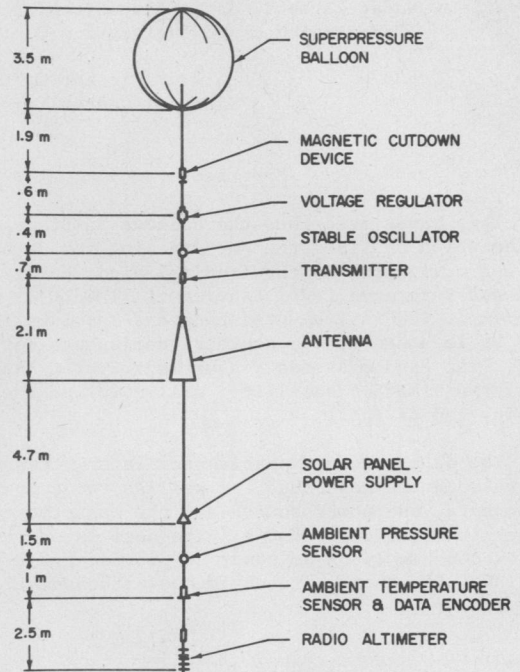


Fig. 2. TWERLE flight train--schematic

logic operates from a +12 V supply and consumes less than 5 mA of current. The complete electrical schematic is shown in Fig. 4. A photograph of the encoder electronics is given in Fig. 5.

The requirements of the TWERLE system call for an accurate time gate in data encoding. To achieve this time accuracy, a crystal oscillator is used as the basic time reference. Countdown and gate circuits are used to derive system timing from the single crystal oscillator frequency. The following timing functions are all derived from the oscillator frequency:

- Bit rate (100 bit/s)
- Digitizing gate times
- Sensor turn-on
- Radio transmission timing
- Fixed format bit pattern generation.

Fig. 6 is the logic diagram of the timing circuit. The circuit generates all the basic timing waveforms; all timing signals are derived by gating outputs from this circuit.

The time sequence of the Data Encoder is shown in Fig. 7 and below:

- (a) Transmitter on - The initial step in the timing cycle is turning on the transmitter for 1 s. Details within this event will be described later.
- (b) Altimeter power on - Immediately following "transmitter on", +12 V are switched to the radio altimeter. The "on" time is 45.44 s.
- (c) Count altitude - The altimeter signal is digitized during the last 2.56 s of "altimeter power on".
- (d) Count air temperature - Air temperature is digitized as follows: down count on a temperature reference for 1.28 s; pause for 1.28 s to allow for the temperature circuit

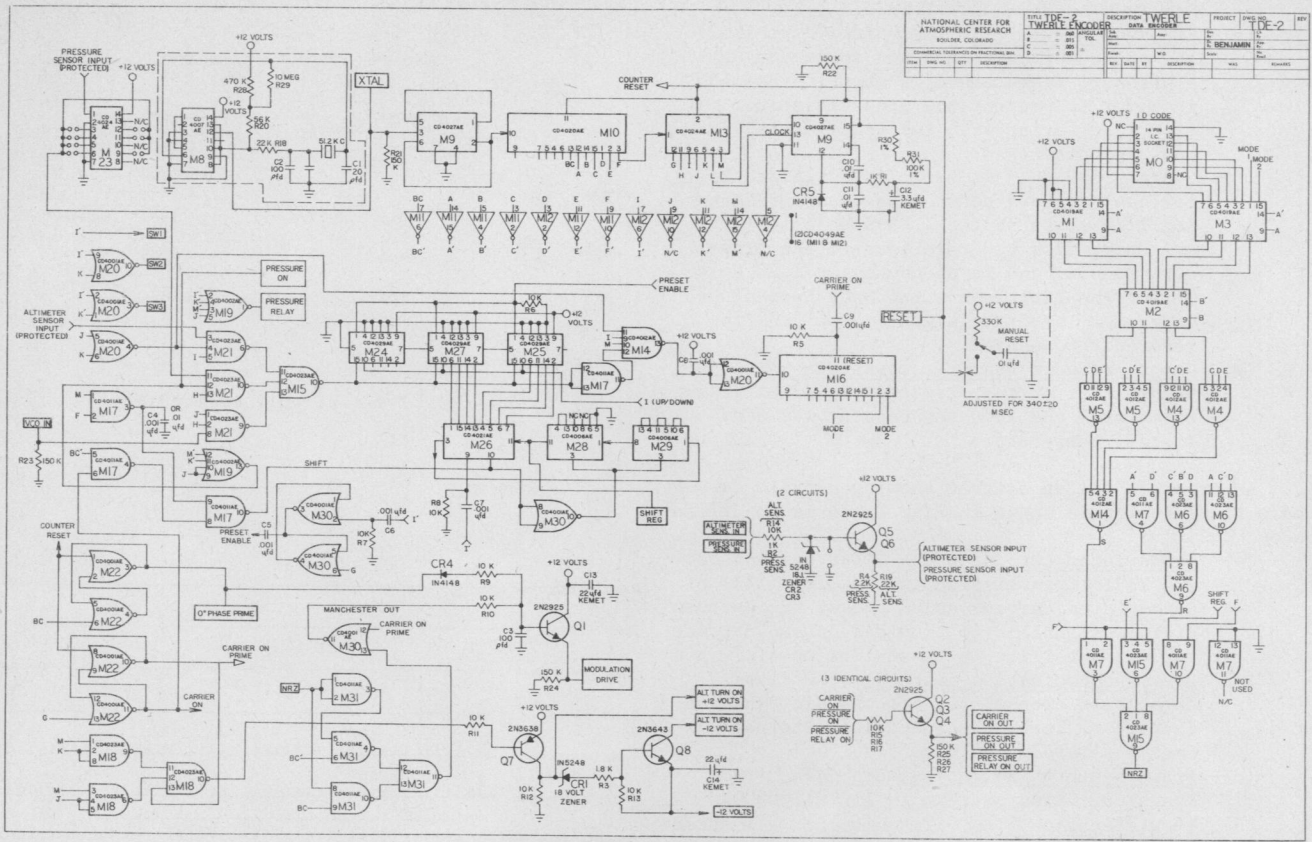


Fig. 4. Data encoder schematic diagram

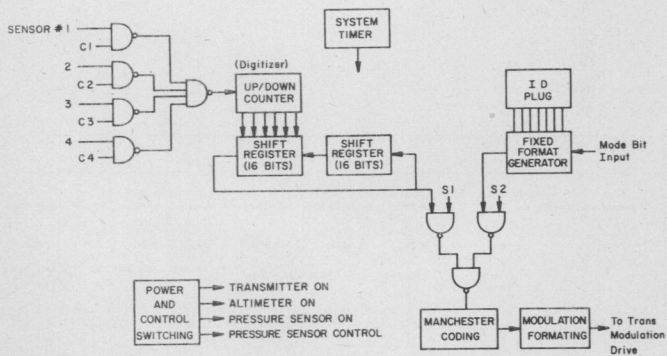


Fig. 3. Data encoder block diagram

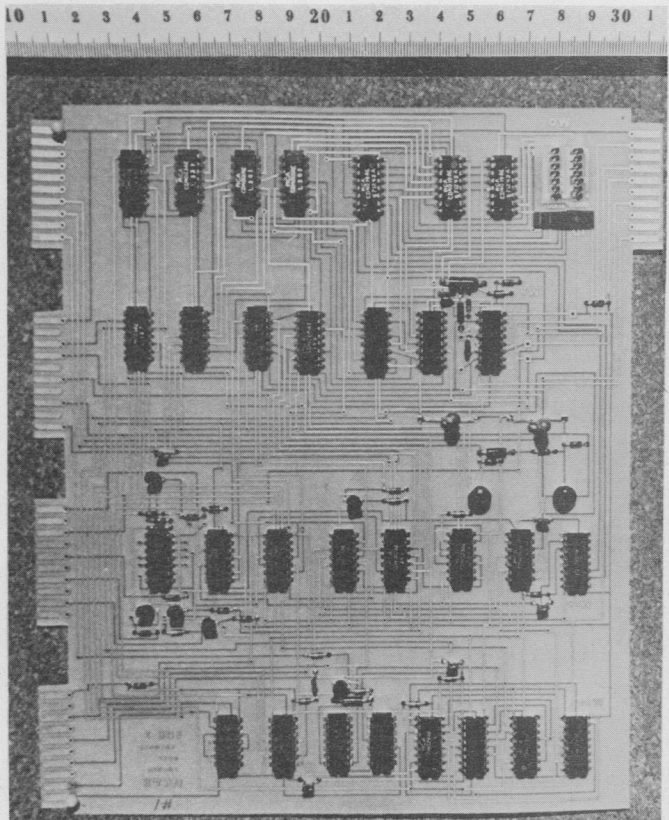


Fig. 5. The TWERLE data encoder

to switch from reference to temperature sensor; and count up for 1.28 s.

- (e) Pressure sensor on - The buffer circuits for the pressure sensor are not turned on until a pressure measurement is about to be made, in order to prevent the pressure sensor from interfering with the temperature measurements.
- (f) Count pressure - Pressure is digitized as follows: a down count on pressure reference for 1.28 s; pause for 1.28 s to allow switching from the reference to the pressure sensor; and an up count for 1.28 s. During the last 2.56 s the Data Encoder provides a relay drive signal to switch from reference to sensor.
- (g) Count pressure sensor temperature - The temperature of the pressure sensor is digitized with the same sequence as was used for air temperature.

An expanded timing diagram showing details during radio transmission is shown in Fig. 8 and is described below:

- (a) Unmodulated carrier - The first portion of the radio transmission is 0.32 to 0.36 s of unmodulated carrier at 0° phase; the purpose of this signal is to provide a clean carrier for the satellite to phase-lock onto.
- (b) Bit synchronization pattern - The first eight bits transmitted are the bit synchronization pattern, a sequence of alternate ones and zeroes (10101010).
- (c) Frame synchronization pattern - The frame synchronization pattern is 110101100000.
- (d) Identification bits - Ten bits are allocated for identification and are determined by an ID plug which is inserted into the Data Encoder P.C. board. Small printed circuit boards are used to wire the ID codes on the plugs. There are 32 different code boards and two boards are used on each plug. The total number of possible codes is  $32^2=1024$ .
- (e) Mode bits - Two bits which were originally designated as mode bits are now used as extra data bits for the radio altimeter.
- (f) Data bits - The last 32 bits contain the sensor data. First eight bits - radio altimeter: Least significant bit first. (Note the radio altimeter is encoded to a total of 10 bits.) The two most significant bits are the mode bits, the first mode bit being less significant than the second. Second eight bits - air temperature: Least significant bit first. Third eight bits - pressure: Least significant bit first. Fourth eight bits - pressure temperature: Least significant bit first.

All of the sensor outputs are frequencies and three of the sensors--pressure, air temperature, and pressure temperature--have references. The reference is a fixed pressure (capacitance) or a fixed temperature (resistor) that is switched into the measuring circuit. The output from the sensor is a frequency which is alternately proportional to the reference value or the sensor value. An up/down counter is used to digitize this type of data. The reference is subtracted from the sensor by the counter and the difference is transmitted. This scheme greatly improves measurement accuracy because errors occurring in the circuits following the sensor are common to both the sensor and reference. Subtraction of reference from sensor measurement nearly eliminates this common error. The up/down counter is 12 binary stages long; only the last eight counter stages, the eight most significant

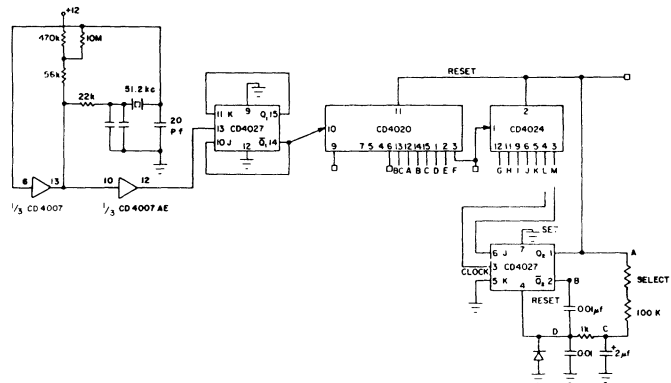


Fig. 6. Timer circuit logic diagram

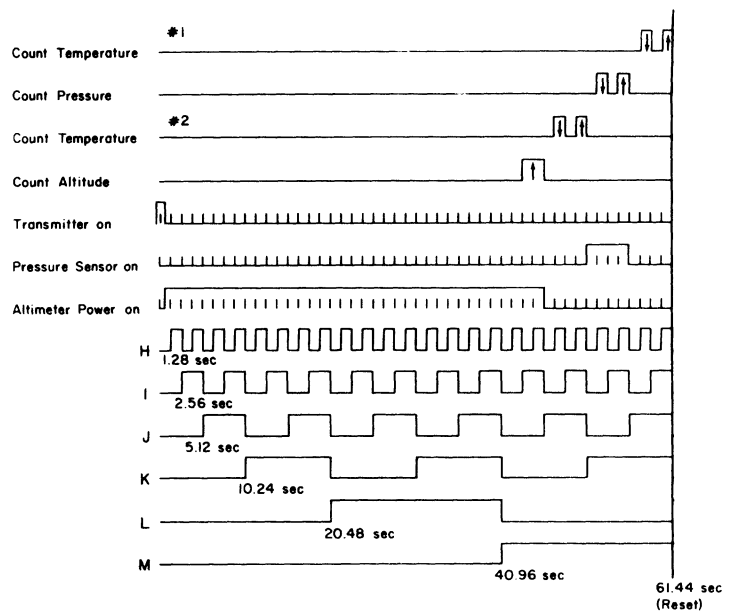


Fig. 7. Data encoder timing diagram

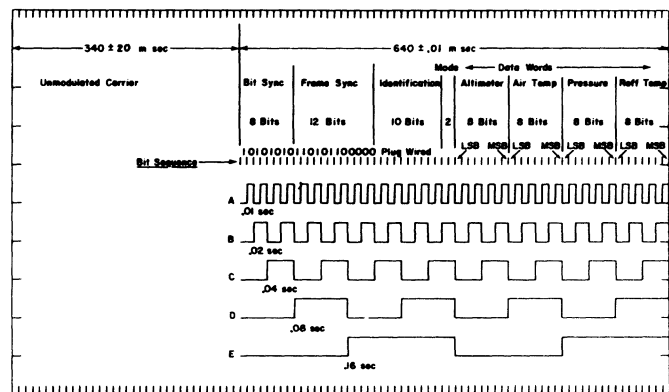


Fig. 8. TWERLE transmission sequence



bits, are read out. The presence of the four unread counter stages almost eliminates the  $\pm$  one bit gating error that occurs when the first stage of a counter is read. The counter is not long enough to hold the complete sensor reading. The most significant bits spill out the end of the counter, leaving only less significant bits for read out. This loss of the most significant bits is acceptable since the experimenter has external methods for determining their value, with the exception of the radio altimeter, where the experimenter requires two more bits to define his reading without ambiguity. To accomplish this, a CD 4020 counter module is added to the circuit; the module provides two additional counter stages beyond the 12-stage up/down counter; these additional bits are read out at the mode bit positions.

After the sensor data is digitized in the counter it is parallel dumped, eight bits at a time, into a shift register, where all 32 data bits are stored at the end of the digitizing sequence.

All of the bit synchronization and most of the frame synchronization bits are generated by an AND/OR gate circuit which uses input signals from the timing circuit. The output from this circuit is labeled "R" (Fig. 4). The circuit whose output is labeled "S" generates the ID code, inserts the mode bits, and generates the four remaining frame synchronization bits.

The ID code is plug-wired. There is one pin connection for each ID bit. Connecting a bit to +12 V produces a "1"; a 0 V connection produces a "0".

The encoder output is Manchester-coded. The Manchester code gives a state transition for every bit. A logic "one" is Manchester-coded as zero at the beginning of an NRZ bit period, shifting to + at the center of the NRZ period. Logic "zero" is + at the beginning of the NRZ bit period, shifting to zero at the center of an NRZ bit period.

The TWERLE system requires three phases of modulation. The transmitter is turned on at zero phase which is transmitted for 0.340 s. During this time the satellite receiver phase-locks onto the carrier; after the acquisition time the Manchester-coded data phase modulates the signal.

Logical One.  $-60^\circ$  at the beginning of an NRZ bit period, shifting to  $+60^\circ$  at center of an NRZ bit period (total transition of  $+120^\circ$ ).

Logical Zero.  $+60^\circ$  at the beginning of an NRZ bit period, shifting to  $-60^\circ$  at center of an NRZ bit period (total transition of  $-120^\circ$ ).

Special Note: The first half-bit of data is held at  $0^\circ$  phase.

The last function of the encoder is power and control switching. Time sequence switching functions are derived from the system timer and are designed to prevent mutual interference and to conserve power.

Transmitter On. The stable oscillator and oven are always on; the rest of the transmitter is turned on only for RF transmission.

Radio Altimeter. Immediately following the RF transmission, the radio altimeter is turned on. The altimeter is given power for 45 s, which gives it time to lock-on and digitize a measurement. The altimeter is turned off at all other times to conserve power and to prevent mutual interference.

Pressure Sensor. To prevent interference with other sensor circuits, the buffer circuit of the pressure sensor is turned on only during the pressure measurement interval. A driver signal which is synchronous with the counter up/down cycle switches the pressure sensor input between the pressure capsule and a reference capacitor.

### Transmitter

The TWERLE transmitter is basically a voltage-controlled power oscillator sample-phase-locked to a crystal oscillator. The operation of the transmitter will be discussed using the block diagram of Fig. 9. The stable 50.15 MHz signal from the crystal oscillator triggers narrow pulses at the sampler, which are then multiplied by a portion of the RF output signal, extracted from the output path by a  $-20$  dB directional coupler. The error signal from the multiplier is amplified and filtered by the loop amplifier before it is applied to a varicap diode which varies the power oscillator frequency around 401.2 MHz. The phase modulation is inserted in the RF section of the feedback path. The modulator utilizes a quadrature hybrid junction phase shifter.

The main advantage of the sampled phase-lock loop approach is its simplicity both in construction and adjustment, compared to the more conventional multiplier chain. It also proves to be more efficient than a multiplier chain<sup>1</sup>. The phase-lock loop also provides a convenient place to insert phase modulation.

Physically, the power oscillator, the directional coupler and the modulator are etched on one microstrip board  $7\frac{1}{2}$ " by  $2\frac{1}{4}$ ", and the sampler, the loop amplifier, the modulator driver and switching circuit are built on a printed circuit board of similar size (Fig. 10). The two boards are attached back-to-back. They are packaged in a rectangular styrofoam box. The crystal oscillator and its oven control circuitry are housed in a separate spherical package.

The power oscillator (Fig. 13) is a microstrip design, grounded collector circuit. The oscillation frequency is determined by a microstrip  $\frac{1}{4}\lambda$  line, with a tap for the emitter. Output is extracted from the base, through a matching network for a 50 Ohm load. Voltage control of the frequency is obtained by a varicap in series with a small decoupling capacitor connected in parallel to the emitter tap. Adjustment of the free running frequency is available, over a range of approximately  $\pm 20$  MHz, by means of a 1.3 pF variable capacitor at the end of the  $\frac{1}{4}\lambda$  line.

A typical free running frequency vs. temperature curve of the power oscillator, with the varicap biased at 0 V, is given in Fig. 11. The frequency stability is better than  $\pm 0.6$  MHz @400 MHz over the temperature range  $-50^\circ\text{C}$  to  $+20^\circ\text{C}$ .

A typical plot of power oscillator output-power and efficiency is given in Fig. 12. The results given are for the CTC transistor type C1-28. Very similar results were obtained for RCA 2N5917, RCA 40941, Motorola 2N6635, and TI 4429. Overall, the transmitter consumes 1.6 W dc power for a 0.6 W modulated RF output.

To guarantee proper oscillations down to  $-40^\circ\text{C}$  a sensistor is included in the biasing circuitry.

The modulator is a quadrature hybrid junction phase shifter with varicap tuned loading elements<sup>2</sup>. Placing the modulator in the feedback path enables operation at an RF level which is 20 dB below the out-

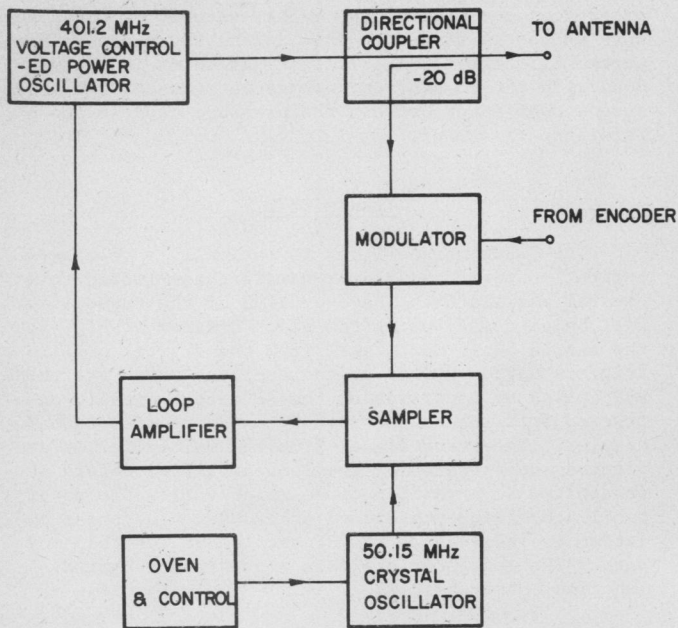


Fig. 9. Transmitter block diagram

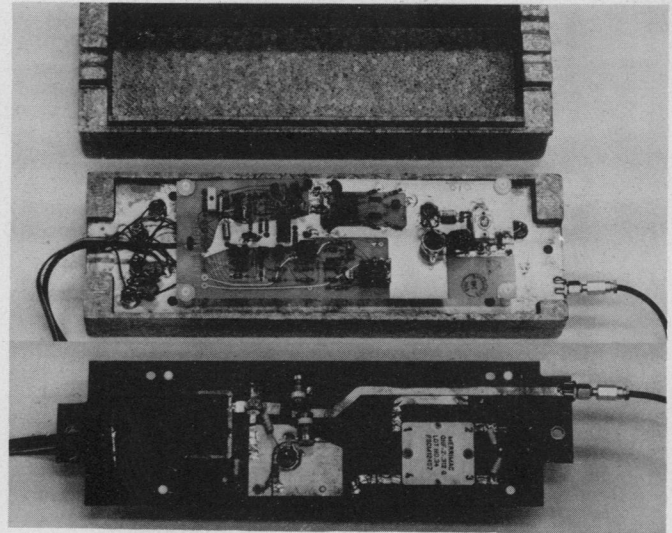


Fig. 10. The TWERLE transmitter

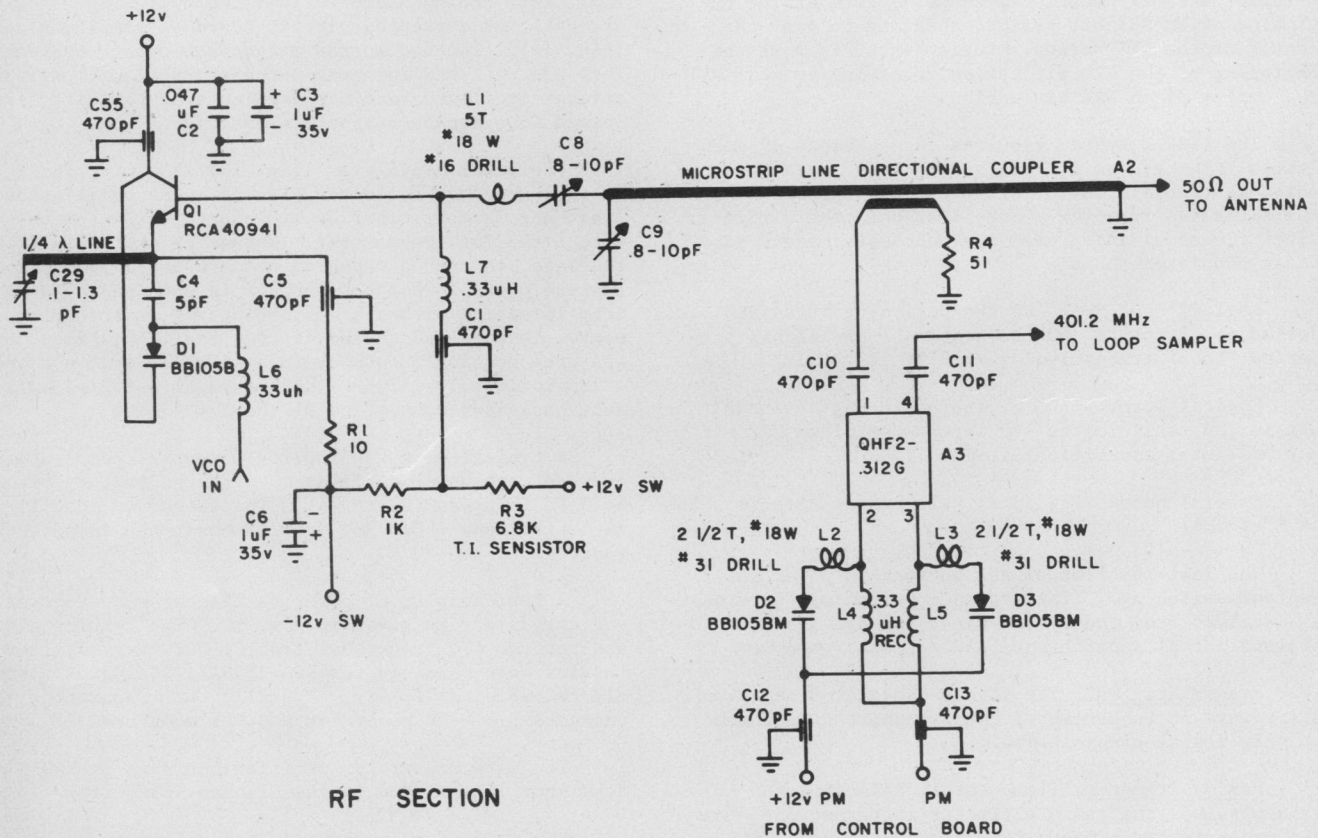


Fig. 13. Transmitter schematic diagram (power oscillator and modulator)

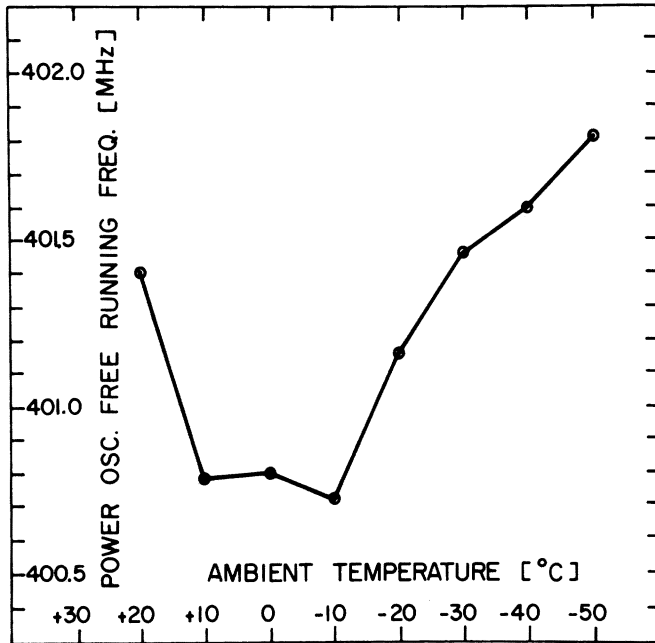


Fig. 11. Free running frequency of the power oscillator vs. temperature

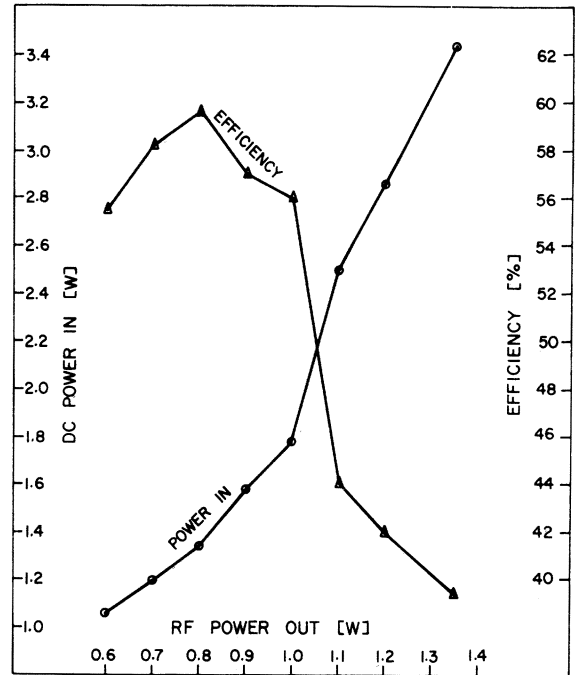


Fig. 12. Efficiency of the power oscillator vs. output power

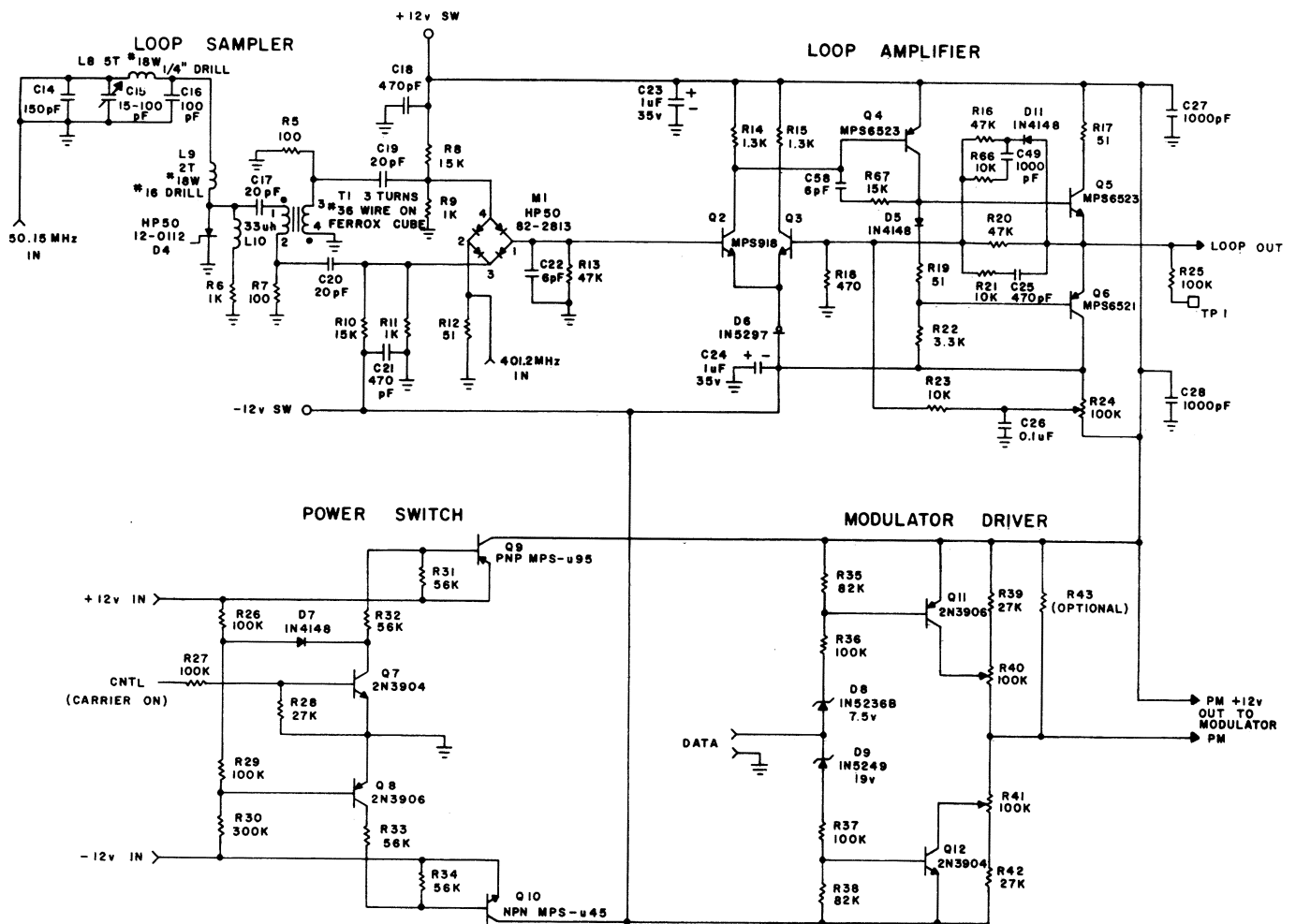


Fig. 14. Transmitter schematic diagram (sampler, loop amplifier, modulator interface and switching)

put level, i.e., 6 mW, resulting in an RF voltage across the varicap which is considerably smaller than the bias. Another inherent result of placing the modulator in the feedback path is that any residual amplitude modulation caused by the modulator does not show up in the output path. The +60, 0, and -60 degrees phase shifts are obtained by applying typically 2V, 8V, and 20V across the varicap.

A modulation driver is used to translate the encoder modulation voltage levels, to the levels required by the modulator. The +60° and -60° levels are adjusted by two potentiometers.

The sampler (see Fig. 14) receives two input signals, the 50.15 MHz signal from the crystal oscillator and the 401.2 MHz signal from the power oscillator. The output of the sampler is a low frequency signal which is related to the phase error between the two inputs.

The sampler is made up of two parts; the sampling pulse generator and the multiplier. A step recovery varactor diode is used to generate the narrow, 1 ns wide, pulses at a rate of 50.15 MHz. These pulses are fed through a ferrite bead transformer to the multiplier, where they multiply the 401.2 signal. The multiplier consists of a biased hot carrier diode quad bridge. The output of the bridge goes to the loop amplifier.

The loop amplifier is a three stage dc amplifier of conventional design. The first stage is a current source stabilized differential amplifier which is followed by a common emitter voltage gain stage. The output stage is a complimentary emitter follower. The open loop amplifier gain is approximately 4000. For negative output voltage, the closed loop dc gain of the amplifier is 100. It is reduced to 50 for positive output voltage, to compensate for the nonlinearity of the varicap. The high frequency gains are 20 and 10, respectively. The transition frequency of the lag-lead filter is near 0.1 MHz.

Typical other parameters of the loop are: phase detector gain  $K_1 = 0.2$  V/rad, average VCO gain  $K_2 = 1$  MHz/V =  $6.28 \times 10^6$  rad/s/V and average loop amplifier high frequency gain  $K_3 = 15$ . The loop gain,  $K$ , is given by

$$K = K_1 K_2 K_3 = 2 \times 10^7 \text{ sec}^{-1} \quad (1)$$

yielding a theoretical "lock in" range  $\Delta f_L$

$$\text{where } \Delta f_L = \frac{K}{2\pi} = 3.2 \text{ MHz} \quad (2)$$

The "lock in" range is the frequency range within which the lock-up occurs without cycle skipping, and the time required to lock-up is less than  $K^{-1}$  seconds, which in our case is 50 ns. The measured "lock-in" range was  $401.2 \pm 3.5$  MHz. Lock-in symmetry is obtained by biasing the free running frequency of the power oscillator off center.

The "lock-in" range achieved is 6 times larger than the maximum deviation of the free running frequency due to temperature (Fig. 11). The "lock-in" range is limited by the phase shifts, particularly in the loop amplifier. The second order nature of the loop is important when one considers phase errors. The phase shifts generated by the modulator are passed to the output through the loop (by a voltage impulse, not a voltage step). The loop has, however, a steady state phase error  $\theta_e$ , which is given by

$$\theta_e = \frac{2\pi\Delta f}{K[\text{dc}]} \quad (3)$$

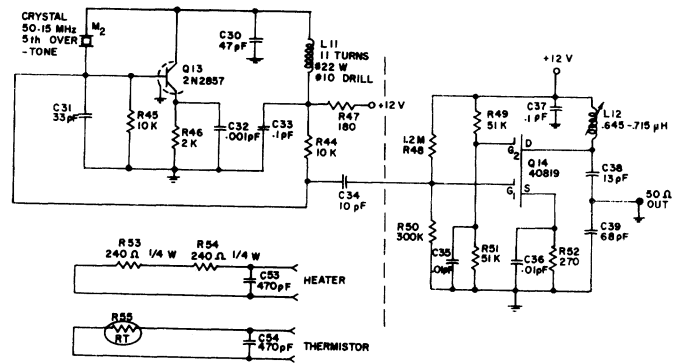


Fig.15. Crystal oscillator and buffer schematic diagram

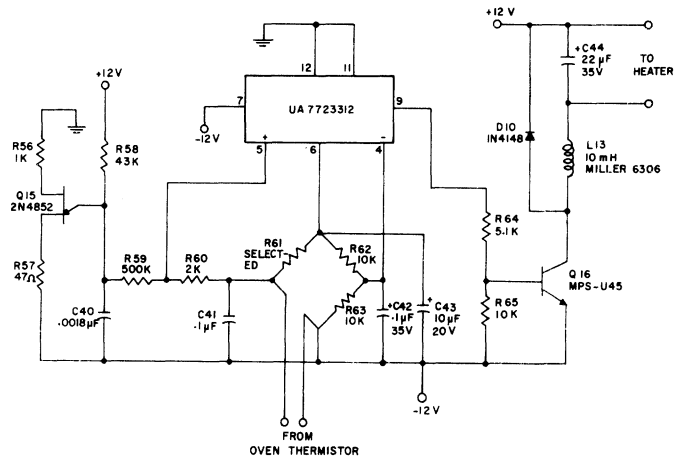


Fig. 16. Oven controller schematic diagram

where  $\Delta f$  is the difference between the free-running frequency and the locked frequency, and  $K[\text{dc}]$  is the loop low frequency gain. Second order effects can cause changes in  $\theta_e$  which may correspond to the modulation signal, and hence comprise a change in the modulation level. Those changes in  $\theta_e$ , as well as  $\theta_e$  itself, are inversely proportional to the loop low-frequency gain. Hence, the higher the gain of the loop the lower the effect of the loop on the modulation. The limit on the loop dc gain is the open loop gain of the loop amplifier (assuming the VCO gain and the phase detector gain are fixed).

### Stable Oscillator

The oscillator provides 50 mW of a stable 50.15 MHz signal to which the 401.2 MHz power oscillator locks. The electrical circuitry consists of three subassemblies: the crystal oscillator, the buffer, and the oven controller. The thermal packaging consists of a miniature Dewar flask, the oscillator-buffer package, and the spherical foam enclosure.

The crystal oscillator (Fig. 15) is a Pierce oscillator operating at 50.15 MHz using a fifth overtone AT cut crystal. The oscillation frequency of the circuit is slightly above the series resonant frequency of the crystal due to the series capacitive load of about 15 pF formed by C31 and the effective capacitance of the tuned collector circuit L11 and C30. The tuned circuit in the collector selects the proper crystal



overtone mode.

A fifth overtone crystal is chosen to provide a small tuning range while maintaining good resistance to frequency pulling. The crystal used has a capacitance ratio,  $r$ , of about 7000 and can be tuned in the circuit over a range of 500 to 1000 Hz at 50 MHz. Tuning is accomplished by decreasing or increasing the inductance via the inter-winding spacing on L11.

The crystal oscillator is coupled to the buffer through a 10 pF capacitor. This small value of coupling capacitance reduces oscillator pulling due to impedance changes at the buffer input. The power consumption of the oscillator is approximately 35 mW.

The RF signal from the crystal oscillator is amplified by a single stage dual gate MOSFET buffer (Fig. 15). The dual gate structure provides lower feedback capacitance, better gain and lower spurious response than possible with a single gate structure. L12, C38 and C39 tune the buffer output and match the output to the load. The buffer raises the RF signal to a level of 50 mW into 50 Ohms and consumes 110 mW from the +12V power supply. The physical size and power dissipation preclude the placement of the buffer inside the Dewar flask active oven. The total power consumption of the oscillator, buffer, oven and oven controller, at typical ambient temperature of  $-30^{\circ}\text{C}$ , is 0.24 W.

The oven controller consists of a 723 voltage regulator IC operated in a pulse width switching mode (Fig. 16). The unijunction transistor Q15, generates a sawtooth at the sampling rate. The thermistor, R55, bonded between the crystal and the heater resistors, alters the bridge output according to the temperature sensed. As the dc output of the bridge changes, the dc pedestal on which the sawtooth rides changes. The 723 switches when the sawtooth exceeds the threshold level. The duty cycle of the switched output depends on the dc output of the bridge. The output of the driver transistor, Q16, is filtered by L13 and C44 producing a dc current proportional to the pulse width.

The temperature of the active oven is set by R61. The value of R61 is chosen so that, with the particular thermistor used, the bridge balances at the desired temperature. R60 sets the gain of the controller. The active oven temperature is set at  $+25^{\circ}\text{C}$ . Typical gain of the oven controller is

$$\frac{\Delta P}{\Delta T_{\text{xtal}}} = 0.2 \text{ W/}^{\circ}\text{C} \quad (4)$$

The oscillator circuitry is housed in a miniature Dewar flask (3 5/8" long, 1" diam). The measured thermal resistance of the flask, including its cork, is

$$\frac{\Delta T_{\text{amb}}}{\Delta P} = 250 \text{ to } 500^{\circ}\text{C/W} \quad (5)$$

Multiplying (4) by (5) we get

$$G = \frac{\Delta T_{\text{amb}}}{\Delta T_{\text{xtal}}} = 50 \text{ to } 100 \quad (6)$$

Typical measured time to complete 63% of the crystal temperature change following a step in ambient temperature is

$$\tau = 40 \text{ min} \quad (7)$$

The closed loop response of the active oven is given by

$$\Delta T_{\text{xtal}}(s) = \frac{\Delta T_{\text{amb}}(s)}{(G+1)(S\tau+1)} \quad (8)$$

where  $G$  and  $\tau$  are given in (6) and (7).

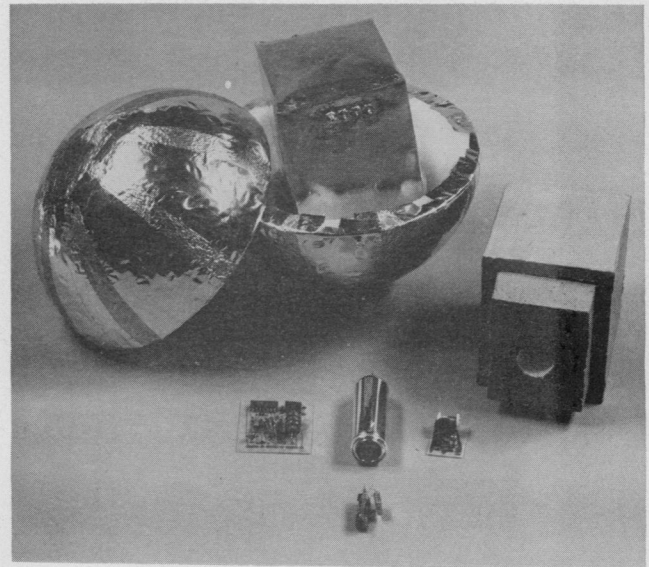


Fig. 17. The TWERLE stable oscillator

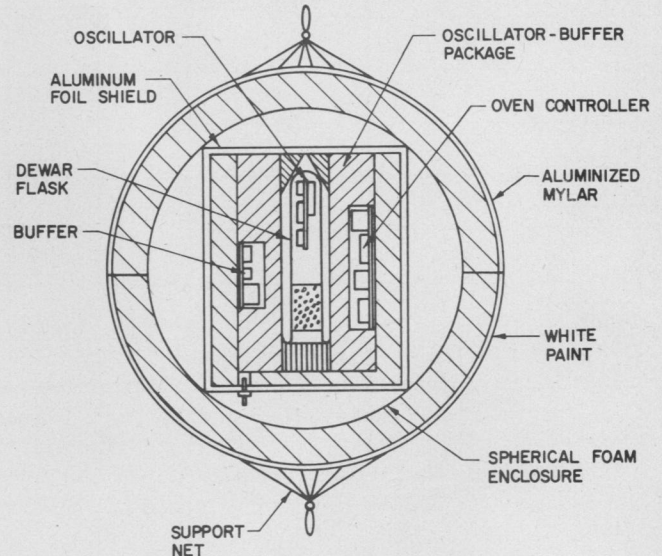


Fig. 18. The stable oscillator packaging

The flask, the buffer and the oven controller are housed in a rectangular foam package (Figs. 17,18) which also serves as a base for an RF shield made of aluminum foil.

To minimize temperature variations vs. sun-angle, the outside package is spherical. White paint (normal absorbtivity/normal emissivity = 0.32) covers the lower hemisphere, and aluminized mylar, with the mylar side out, ( $\alpha_n/\epsilon_n = 0.5$ ) covers the upper hemisphere. Typical temperatures inside such a spherical passive package, as taken during three different balloon flights, are given in Fig. 19. The highest rate of change was for balloon TZ03 between 12:00 and 13:00. The temperature change during this hour was  $8^{\circ}\text{C}$ . It should be noted that from the balloon-borne radar altimeter it is known that this balloon has crossed from ocean to land at 11:58. The typical balloon altitude during these flights was 13.5 km, and the typical ambient temperature was  $-55^{\circ}\text{C}$ .

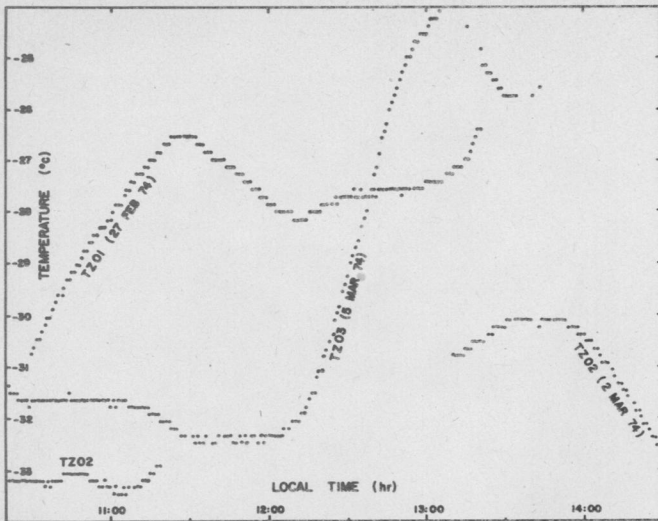


Fig. 19. Temperature behaviour of the oscillator passive packaging

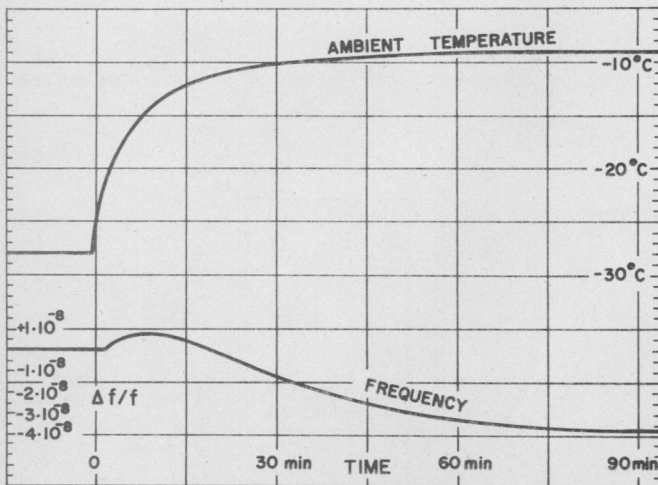


Fig. 20. Oscillator frequency vs. ambient temperature step

Such an 8°C ramp lasting 60 minutes will result in maximum crystal temperature change (inside a 250°C/W Dewar) of 0.03°C/15 min. To meet the frequency stability requirement which is  $\pm 10^{-8}/15$  min will require a crystal with a temperature slope better than  $\pm 0.3$  ppm/°C. Low-cost AT cut crystals can meet a requirement of  $\pm 0.1$  ppm/°C over the range +20°C to +30°C. Setting the oven temperature in the middle of this wide range eliminates the need for resistor selection in the temperature determining bridge, hence simplifying mass production.

A typical frequency change as a result of a 20°C step in the ambient temperature is given in Fig. 20. The long time-constant phenomena (decrease of  $5 \times 10^{-8}$  in 90 min) is due to the change in crystal temperature as discussed above. The short time-constant phenomena (increase of  $1 \times 10^{-8}$  in 8 min) is due to frequency pulling by the buffer which is practically exposed to ambient temperature.

## Antenna

The balloon-to-satellite antenna is a four arm equiangular conical spiral operating in mode two<sup>3</sup>. The antenna is designed for maximum gain at an angle of  $\theta = 75^\circ$  off the cone axis. The antenna parameters are summarized below:

- $\theta_0$  = half the cone angle =  $10^\circ$
- D = base diameter = 59.6 cm (0.797λ)
- d = top diameter = 8.7 cm (0.116λ)
- $\alpha$  = angle between the radius vector and a tangent to the log-spiral curve at point of intersection =  $52^\circ$
- $\delta$  = arm width  $45^\circ$

A measured radiation pattern vs. elevation angle is given in Fig. 21. The radiation pattern vs. azimuth (not shown) is only quasi-circular (as in Figs. 8, 9 in<sup>3</sup>) with a difference of 3 dB between maxima and minima, measured at  $\theta = 75^\circ$ . The azimuthal variation could be reduced only through a considerable increase in the antenna dimensions.

A printed circuit balun<sup>4</sup> was used to unbalance and match the antenna impedance to a 50 Ω coaxial line. The match is obtained by adding another microstrip in parallel to the microstrip used as the transmission line between the input of the balun and the load. The added microstrip is used as a tuning stub. A VSWR of less than 1.15 was easily attained in mass production of the antenna and balun. Successive crushing and redeployment of the antenna did not affect the VSWR by more than  $\pm 5\%$ .

Mechanically the antenna weighs only 150 g; yet it is rugged and instantly deployable. There are three basic parts to the antenna--the outer skin, a supporting skelton and an apex assembly (Fig. 22).

The outer skin is the functional part of the antenna. It is conical in shape, and is composed of clear one-third mil thick polyester film onto which

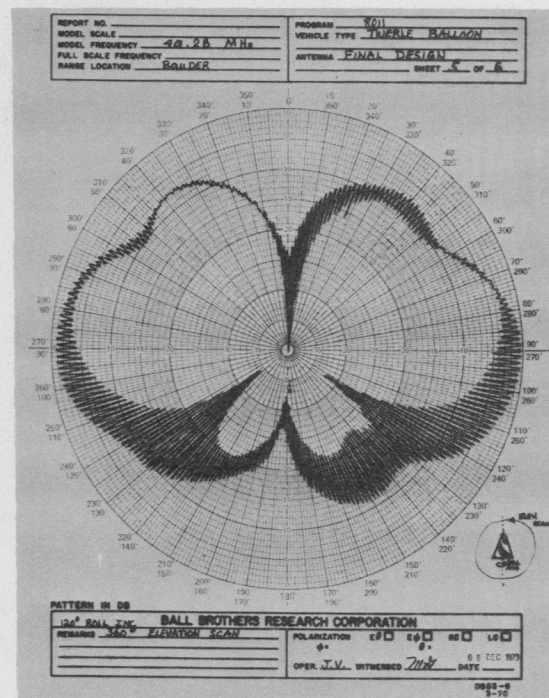


Fig. 21. Radiation pattern of the TWERLE conical spiral antenna



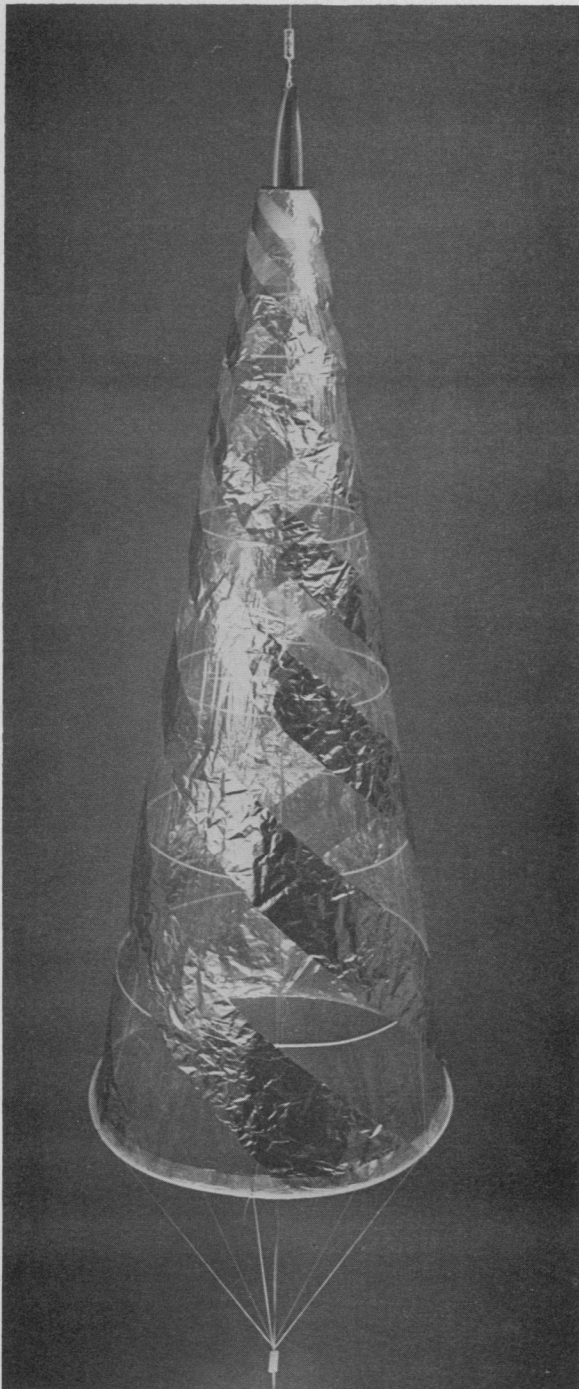


Fig. 22. The TWERLE conical spiral antenna

logarithmically tapered antenna elements are laminated. These elements consist of quarter-mil thick spiraling aluminum foil stripes.

The supporting skeleton is composed of five nylon hoops suspended in a conical fashion by six dacron cords. Before deployment, the antenna appears as a shapeless mass of plastic film. However, upon launch when tension is applied across the skeleton, the antenna skin is instantly deployed and takes on its conical form. It should be noted that only the bottom hoop is attached to the skin, with the connecting cords between the bottom hoop and the one above it slightly too long. In this way the weight of the remaining flight train is carried by the skin, causing it to pull

tight.

The rigid apex assembly provides the means to mechanically suspend the antenna. The apex houses the balun and provides a solid mechanical base for making electrical connection to the fragile outer conical skin.

#### Power Supply

Power for the system is provided directly from a solar panel. Rechargeable batteries were considered during the planning of TWERLE but were discarded when it was decided that the power consumed by the various components in the flight train could be time-sequenced so that there were no peak loads that a solar panel could not handle. The solar power supply provides +12 V and -12 V and is capable of delivering 90 to 150 mA, depending on the elevation angle of the sun. At an altitude of 14 km, where TWERLE balloons fly, attenuation of the solar input due to clouds is rarely a problem.

The solar array is constructed from three equilateral panel sections that are joined together at the edges to produce a three-sided pyramid (see Fig. 23). This shape of array does not produce the maximum power averaged over the day. Its advantage is that it produces a nearly constant power for all solar elevation angles. The optimum shape for maximum average power is a single flat panel. For all angles above 20°, the flat panel produces more power than the pyramidal shape. Fig. 21 shows the comparison between the flat array and the pyramid-shaped array. Two design innovations were incorporated to get extra power from the solar array. One of these was to place a reflective white styrofoam disc at the bottom of the pyramid. At high solar elevation angles the disc reflects sufficient light to the panels to produce 40% additional power. The white surface is a diffuse reflector. A mirror reflector was considered but tests showed that its performance was highly angle-dependent and that it did not uniformly illuminate the solar panel.

The second innovation was to open the bottom and top of the pyramid structure to provide air ventilation through the pyramid. The voltage producing capability of a solar cell decreases with temperature. By providing ventilation through the center of the panel, the cell temperature is reduced to approximately +10°C. Without internal ventilation the cells would run at approximately +50°C and produce 15% less voltage.

Each panel contains 60 N on P, 2 cm x 2 cm silicon cells. A single cell produces 100 mA at 0.465 V under one sun illumination. The complete panel produces 27.30 V. The panel is center-tapped and the output is voltage-regulated to +12 V and -12 V. A shunt-type voltage regulator is used. The regulator simply consumes whatever power is required to hold the voltage down to 12 V. The shunt-type regulator saves cells since it is not necessary to provide the voltage drop across a conventional series regulator.

The cells are assembled on a 7 mil thick PC board. Each cell is connected to the board by four small (#30 gauge) buss wires. The wires have strain relief bends so each cell is suspended at its corners by a thin wire. This protects the cells from breakage due to PC board flexure.

Before the completed panels are tested, they are thermally cycled three times to -80°C. This extreme cycling breaks the weak and stressed cells.

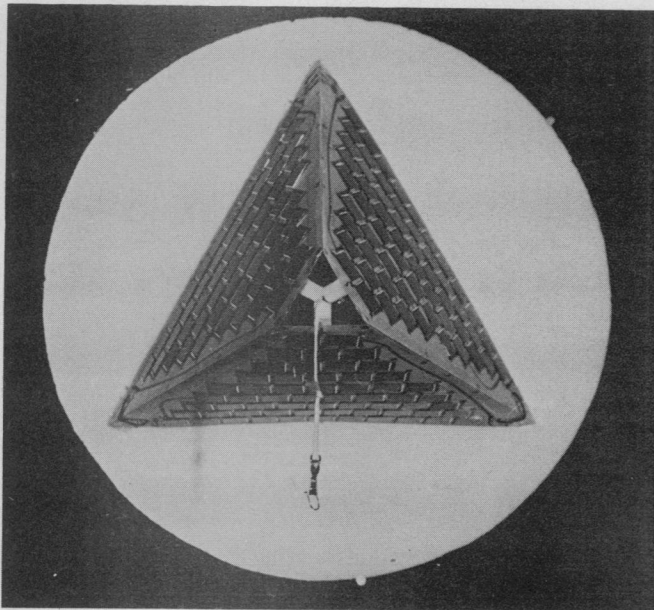


Fig. 23. The TWERLE solar panel

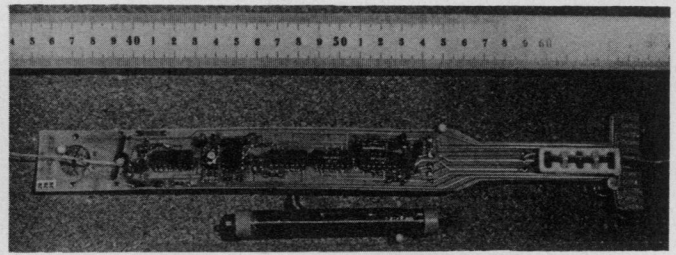


Fig. 25. The TWERLE magnetic cutdown device

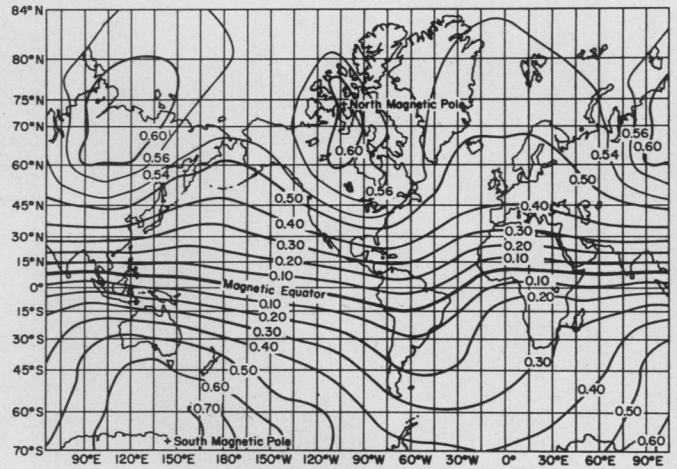


Fig. 26. Map of vertical intensity of the Earth's magnetic field expressed in Gauss

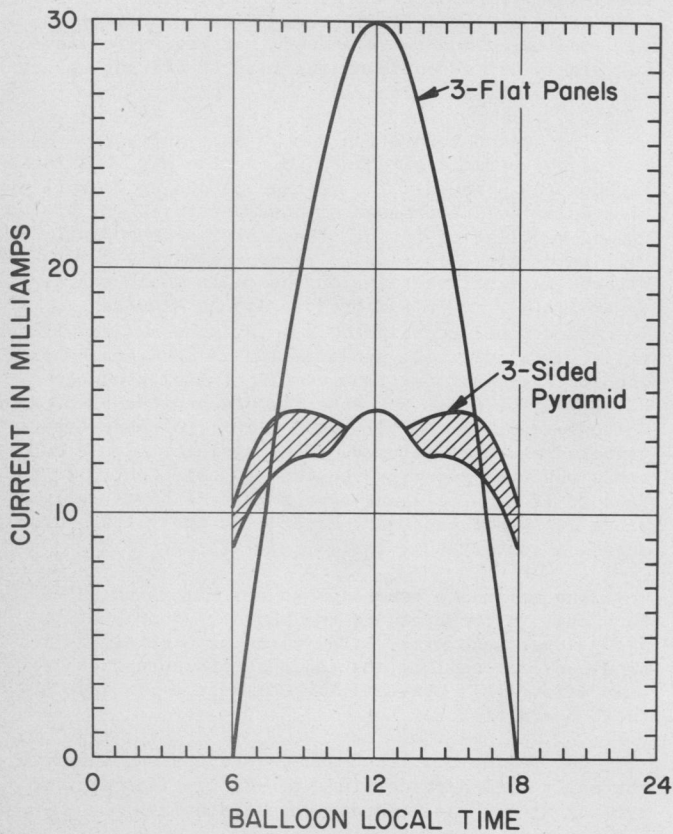


Fig. 24. Power vs. sun angle

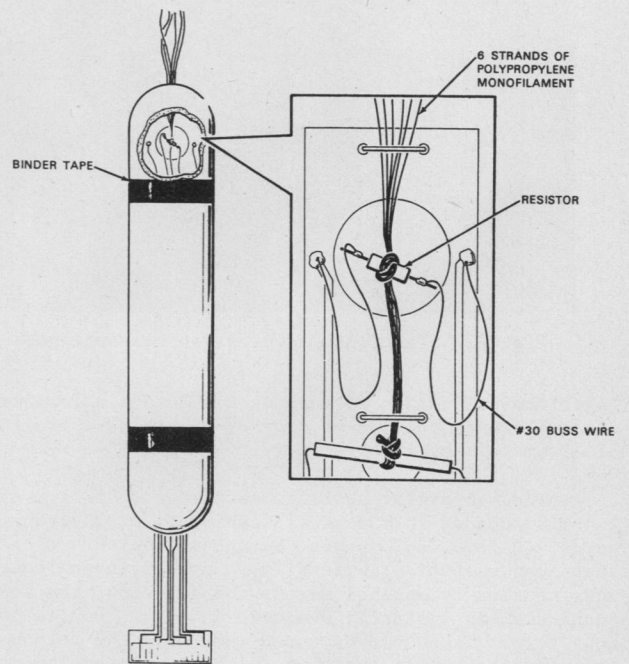


Fig. 28. Expanded view of cutdown mechanism

### Magnetic Cutdown Device

Several northern hemisphere countries will not allow balloon overflight. A cutdown device is therefore required to terminate the flight of any TWERLE balloon before it flies beyond the tropics into the northern hemisphere. The cutdown mechanism should not be hazardous to aircraft, should not contain explosives, should be lightweight, and should operate with low electrical power. These requirements are met by the cutdown device described below (see Fig. 25).

The basic element of the cutdown device is a simplified flux gate magnetometer which senses the vertical component of the earth's magnetic field. This field component is at a maximum at the magnetic poles and passes through zero at the magnetic equator. Fig. 26 is a map of the vertical component of magnetic field intensity. The polarity of the field is positive in the northern hemisphere and negative in the southern hemisphere.

Such a magnetic cutdown device can be set to operate at any desired field intensity; for the TWERLE program it has been set at +0.25 G. When a balloon moves north of this delineation the cutdown system separates the flight train from the balloon.

#### Magnetic sensor

The magnetic sensor is composed of three coils: a drive coil, a pick-off coil, and a long solenoid. The coils are wound on very thin, lightweight plastic coil forms; the drive and pick-off coils are actually wound on plastic soda straws. The three coils are mounted concentrically. A 2 mm thick Dupont "Kapton" printed circuit board is used to connect the delicate wires from the coil windings to the main circuit board. A magnetic core is placed inside the drive coil. The core is fabricated from a G-L Industries, Inc. Magna-Shield H strip, which has a high magnetic permeability and a low magnetic saturation level. The drive coil has two windings, one on each end, connected in phase opposition. When an ac signal is applied across the drive coil, the two ends of the magnetic core are magnetized in phase opposition. The ac drive signal is large enough to drive the core ends into magnetic saturation on each half-cycle. If a biasing magnetic field is present, such as that of the earth, one end of the core goes into saturation sooner than the other. This causes an unbalanced alternating magnetic field that has energy at the second harmonic of the drive frequency. If a pick-off coil is placed around the drive coil, it can detect the second harmonic. The pick-off coil has a capacitor in parallel to tune the coil to resonate at the second harmonic frequency. The relative positions of the drive coil and the magnetic core are adjusted to null the drive signal frequency measured across the pick-off coil; when properly adjusted, the output from the pick-off coil is a sine wave at the second harmonic of the drive frequency. When oriented with a maximum north magnetic field, the sine wave is in phase and has a maximum amplitude of approximately 0.1 V per 0.1 G. Reversal of the sensor orientation causes the output phase to reverse.

Basically the magnetometer sensor and circuit respond to the zero intensity level. However, the cutdown point can be set at any level desired by passing the proper amount of current through the long solenoid that encloses the drive and sense coil; this produces a biasing magnetic field that offsets the zero level. The magnetic field produced in air by a long solenoid is expressed by the equation:

$$H = \frac{4\pi nI}{10} \quad (9)$$

where H = field intensity in G  
n = turns/cm  
I = current in A

#### Electronic circuit

The electrical schematic of the magnetic cutdown is shown in Fig. 27. This circuit consists of the following components:

1. Free-running oscillator
2. Frequency divider
3. Phase comparator
4. Time delay
5. Cutdown mechanism

The oscillator and frequency divider combination provides the drive signal for the magnetic sensor and a reference frequency for the phase comparator.

The phase comparator compares the phase of the second harmonic output from the sense coil with a reference square wave. In the southern hemisphere the two waveforms are in phase opposition. The phase comparator output is a "prevent cutdown" signal. However, north of the magnetic equator the two waveforms are in phase and the phase comparator output turns on a time-delay circuit.

The time-delay circuit provides a 30-s delay to prevent accidental activation in handling the cutdown. It consists of a 14-stage counter that is driven by a unijunction oscillator.

The cutdown mechanism activates when the last stage of the counter goes positive. 24 V are switched across a 1/8-W 330-Ω metal film resistor. The separation mechanism consists of six strands of polypropylene monofilament knotted around the metal film resistor (Fig. 28). The polypropylene has a low melting temperature and a high tensile strength. When cutdown power is applied to the resistor, it is heated and it melts the line in two. This cutdown device operates at 0.3 W and contains no explosives. Insulative foam is packed around the resistor to contain the heat. The resistor leads are replaced with a fine wire (#30 gauge) to reduce thermal conduction.

#### Concluding Remarks

440 units of each of the above instruments have already been manufactured and are awaiting launch. Cost and weight breakdown are as follows: Encoder, \$240, 150 g; transmitter plus stable oscillator, \$290, 315 g; antenna, \$120, 150 g; solar panel and regulator, \$260, 180 g; and magnetic cutdown, \$70, 60 g.

An extensive pre-launch test system has also been built. The test system checks critical parameters with the instruments connected into the flight train. Among the parameters checked are: encoder's fixed format, transmitter's RF power, VSWR, phase modulation levels and free running frequency, and the solar panel output voltages.

Five balloon flights with the complete TWERLE flight train were conducted, in which a receiver similar to the satellite receiver was used on the ground (Boulder, Colorado, September 1973, and Christchurch, N.Z. March 1974). In all of these flights data was received up to the electromagnetic horizon.



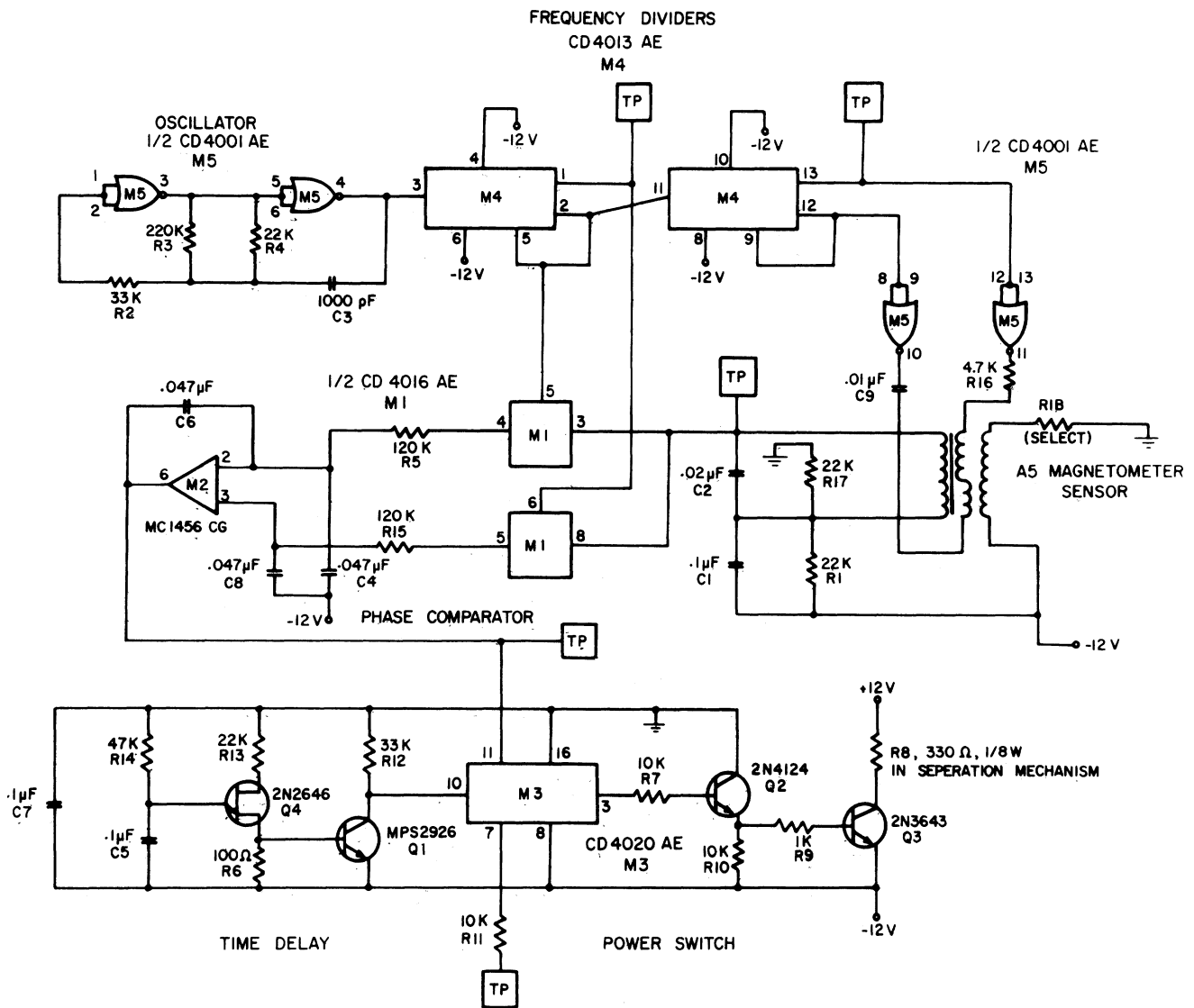


Fig. 27. Magnetic cutdown schematic diagram

Acknowledgements

The information upon which this publication is based was obtained during the Tropical Wind, Energy conversion and Reference Level Experiment (TWERLE) supported by the National Aeronautics and Space Administration and the National Science Foundation administered under the University Corporation for Atmospheric Research contract with the National Science Foundation.

The authors wish to acknowledge the contribution of the late Charles D. Blair III, and the late John A. Kruse to the development and testing of the TWERLE system.

References

1. R.F. Source Co.: "Feasibility study for TWERLE stable oscillator and transmitter package", Final report for contract NCAR-14-72. 1972.
2. R.H. Hardin, E.J. Downey and J. Munushian: "Electronically-variable phase shifter utilizing variable capacitance diodes," Proc. IRE, vol. 48, May 1960, pp. 944-945.
3. J.D. Dyson and P.E. Mayes: "New circularly-polarized frequency-independent antennas with conical beam or omnidirectional patterns," IRE Trans. on Antennas and Propagation, vol. AP-9, July 1961, pp. 334-342.
4. R. Bawer and J.J. Wolfe: "A printed circuit balun for use with spiral antennas," IRE Trans. on Microwave Theory and Techniques, vol. MTT-8, May 1960, pp. 319-325.